Electron Release and Proton Acceptance Reactions of (dpp-BIAN)Mg(THF)$_3$

Igor L. Fedushkin[a], Valentina A. Chudakova[a], Markus Hummert[b], and Herbert Schumann[b]

[a] G. A. Razuvaev Institute of Organometallic Chemistry, Russian Academy of Sciences, Tropinina 49, 603950 Nizhny Novgorod, GSP-445, Russia
[b] Institut für Chemie, Technische Universität Berlin, Straße des 17. Juni 135, D-10623 Berlin, Germany

Reprint requests to Prof. Dr. H. Schumann. Fax +49 30 31422168.
E-mail: schumann@chem.tu-berlin.de

Z. Naturforsch. **2008**, *63b,* 161 – 168; received September 12, 2007

(dpp-BIAN)Mg(THF)$_3$ (**1**) (dpp-BIAN = 1,2-bis[(2,6-diisopropylphenyl)imino]acenaphthene) and $(PhCOO)_2$ react with splitting of the peroxide bridge and formation of the dimeric magnesium benzoate [(dpp-BIAN)MgOCOPh(THF)]$_2$ (**2**). The reaction of **1** with PhCOOH yields the dimeric magnesium benzoate [(dpp-BIAN)(H)MgOCOPh(THF)]$_2$ (**3**), whereas **1** and furanyl-2-carboxylic acid react with liberation of hydrogen and formation of (dpp-BIAN)Mg[OCO(2-C_4H_3O)]$_2$Mg(dpp-BIAN)(THF) (**4**). Compounds **2**, **3**, and **4** have been characterized by elemental analysis, IR spectroscopy, and X-ray structure analysis, compound **3** also by ^{1}H NMR spectroscopy. The eight-membered metallacycles of the centrosymmetric dimers **2** and **3** are almost completely planar. The two magnesium atoms in **4** show different coordination spheres; one is surrounded by its ligands in a trigonal bipyramidal manner, the other one in a tetrahedral fashion. The Mg···Mg separations in **2**, **3** and **4** are 4.236, 4.296, and 4.030 Å, respectively.

Key words: Magnesium, Carboxylates, Diimine Ligands, Crystal Structure Determination

Introduction

Metal complexes with ligands which are able to adopt different valence states like 1,2-diimines, ketimines, and semiquinones (SQ) show quite specific properties, as for instance the reversible intramolecular metal-to-ligand electron transfer in transition metal complexes of *o*-benzosemiquinones (SQ) [1] or the reversible uptake of oxygen by triphenylantimony amidophenolate affording the endoperoxide (Scheme 1) [2].

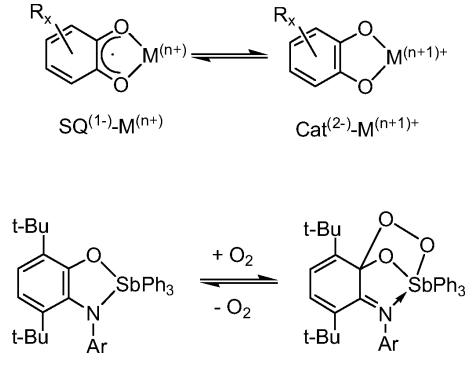

Scheme 1. Redox isomerism in transition metal SQ complexes, and reversible addition of oxygen by triphenylantimony amidophenolate.

In the last few years, we reported on the preparation of alkali and alkaline earth metal complexes containing the diimine ligand 1,2-bis[(2,6-diisopropylphenyl)imino]acenaphthene (dpp-BIAN) in different oxidation states. Thus, the reactions of dpp-BIAN with lithium and sodium in diethyl ether afford mono-, di-, tri-, or tetraanions of the dpp-BIAN ligand depending on the ratio of the reactants and the reaction conditions [3]. The reactions of dpp-BIAN with magnesium and calcium produce complexes containing the ligand as dianion like in (dpp-BIAN)Mg(THF)$_3$ (**1**) and (dpp-BIAN)Ca(THF)$_4$ [4]. In the presence of AlX_3, also aluminum reacts with dpp-BIAN forming the complexes (dpp-BIAN)$^{n-}$AlX$_m$ (n = 1, m = 2; n = 2, m = 1; X = Cl, I) in which the ligand adopts the oxidation state of a monoanionic radical or a dianion [5]. Furthermore, dpp-BIAN complexes of Al(III) [6] and Ge(II) [7] have been prepared by reacting aluminum and germanium halides with dpp-BIAN complexes of the alkali and alkaline earth metals.

0932–0776 / 08 / 0200–0161 $ 06.00

These complexes of the main group metals can act as electron traps as well as electron providers. Thus, the single electron transfer from (dpp-BIAN)Mg(THF)$_3$ (**1**) to Ph_2CO and 9-(10H)-anthracenone affords the dinuclear pinacolate and the quanthranyloxy derivative, respectively (Scheme 2) [8].

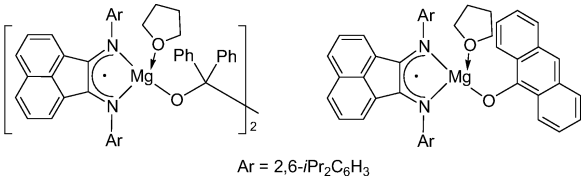

Scheme 2. dpp-BIAN radical-anion derivatives of magnesium.

Also the reactions of **1** with EtX (X = Cl, Br, I) and Me_3SiCl proceed with transfer of one electron from **1** to the respective reactant, producing ethyl and trimethylsilyl radicals which then attack the ligand. In the reaction with Me_3SiCl, additionally the cleavage of a THF ring takes place (Scheme 3) [9]. These reactions proceed in the way of a 1,3-addition of the substrate to the C-N-M fragment of the magnesium complex.

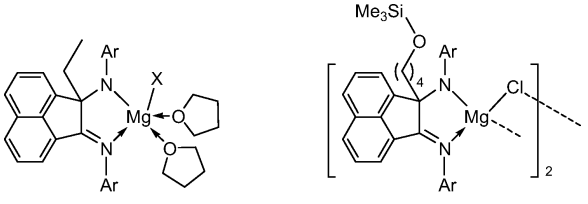

Scheme 3. Products of addition of alkyl and trimethylsilyl halides to the dpp-BIAN dianion of **1**.

Whereas in the above cited reactions of **1** the dpp-BIAN ligand delivers an electron and becomes oxydized from the dianionic to the monoanionic radical state, the opposite process is observed when (dpp-BIAN)$^{\bullet-}$Mg(*i*Pr)(Et_2O) is dissolved in THF. The complex which is quite stable in hydrocarbons and diethyl ether decomposes in THF with reductive elimination of isopropyl radicals and formation of **1** [10].

A further characteristic feature of compound **1** is its ability to add CH-acidic substances as for instance phenylacetylene [11a] and enolisable ketones [11b] and nitriles [11c]. The nucleophilicity of the nitrogen atoms of the dianionic dpp-BIAN ligand in **1** allows an easy uptake of the proton of the respective substrate yielding the corresponding alkinyl, enolate and ketenimate derivatives (Scheme 4).

In this paper we report on the reactions of **1** with benzoyl peroxide, benzoic acid and furanyl-2-carboxylic acid which again illustrate the different facets in the reactivity scale of **1** towards organic substrates.

Results and Discussion

*Synthesis of [(dpp-BIAN)MgOCOPh(THF)]$_2$ (**2**), [(dpp-BIAN)(H)MgOCOPh(THF)]$_2$ (**3**), and (dpp-BIAN)Mg[OCO(2-C_4H_3O)]$_2$Mg(dpp-BIAN)-(THF) (**4**)*

Treatment of **1**, dissolved in THF, with 0.5 equiv. of benzoyl peroxide causes an immediate change in the color of the solution from green-brown, which is characteristic for the dianionic $[(dpp\text{-}BIAN)]^{2-}$ ligand in **1**, to cherry-red, the color which indicates the formation of radical-anionic $[(dpp\text{-}BIAN)]^{\bullet-}$. The isolation of red-brown, crystalline [(dpp-BIAN)-MgOCOPh(THF)]$_2$ (**2**) proves this transfer of an electron from the dpp-BIAN ligand in **1** to the organic reactant according to the change in the oxidation state of the dpp-BIAN ligand from the di- to the mono-anion and the reduction of the peroxide to benzoate anions (Scheme 5). The dimeric complex **2** is sensitive against moisture and air, is only poorly soluble in diethyl ether, but moderately soluble in benzene and toluene, and melts at 157 °C without decomposition.

The reaction of **1** with one equiv. of benzoic acid in THF proceeds very smoothly at r. t. The reaction is accompanied by a change in the color of the solution from green-brown to deep blue, the color which indicates the formation of singly protonated dpp-BIAN ligands (Scheme 4). The isolation of [(dpp-BIAN)-(H)MgOCOPh(THF)]$_2$ (**3**) from diethyl ether as deep blue, almost black crystals confirms the formation of

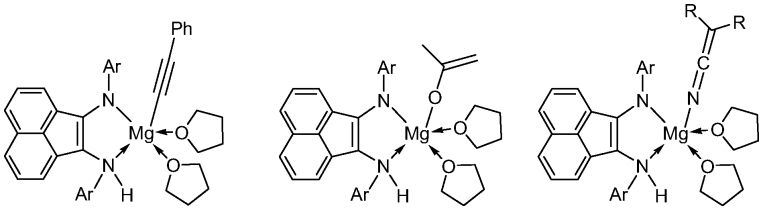

Scheme 4. Products of addition of CH-acidic substances to the dpp-BIAN dianion in **1** (Ar = 2,6-*i*Pr$_2$C$_6$H$_3$).

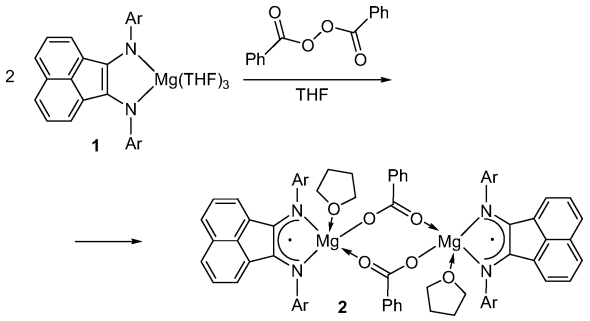

Scheme 5. Reaction route for the synthesis of **2** (Ar = 2,6-*i*Pr$_2$C$_6$H$_3$).

the amino-amido ligand (Scheme 6). Complex **3** is sensitive against moisture and air, and soluble in ethereal solvents and aromatic hydrocarbons. It is thermally stable up to 220 °C.

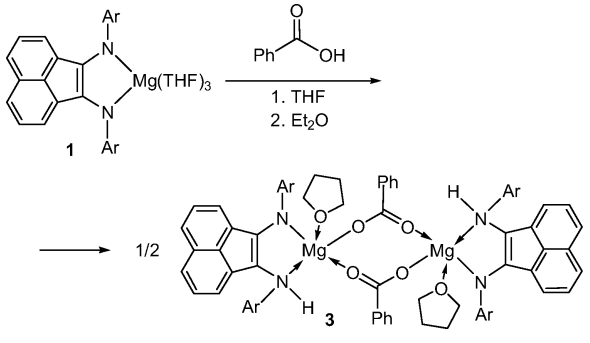

Scheme 6. Reaction route for the synthesis of **3** (Ar = 2,6-*i*Pr$_2$C$_6$H$_3$).

In contrast to the above reaction, treatment of **1** with one equiv. of furanyl-2-carboxylic acid in THF does not cause a deep blue color of the reaction mixture, but a change in color from green-brown to grayish-green. Substitution of the solvent THF by benzene results in the formation of a red-brown solution, from which (dpp-BIAN)Mg[OCO(2-C$_4$H$_3$O)]$_2$-Mg(dpp-BIAN)(THF) (**4**) crystallizes as red crystals, the color which proves the presence of mono-anionic dpp-BIAN radicals (Scheme 7). Complex **4** is sensitive against moisture and air, and only slightly soluble in diethyl ether, but moderately soluble in benzene, toluene and tetrahydrofuran. No decomposition was observed up to 210 °C.

Although the ESR signals of the paramagnetic compounds **2** and **4** are rather broad at r. t., their hyperfine structure, a quintet for both, reflects the coupling of the unpaired electron with the two ^{14}N nuclei of the radical-anionic dpp-BIAN ligand. The signal broadening may be explained by the fluxional behavior of the electrons associated with the carboxylate bridge-mode isomerization discussed below.

*Molecular structures of [(dpp-BIAN)MgOCOPh (THF)]$_2$ (**2**), [(dpp-BIAN)(H)MgOCOPh(THF)]$_2$ (**3**) and (dpp-BIAN)Mg[OCO(2-C$_4$H$_3$O)]$_2$Mg(dpp-BIAN)(THF) (**4**)*

Crystals of **2**, **3**, and **4** suitable for single crystal X-ray diffraction were obtained from THF, Et$_2$O, and benzene, respectively. Compounds **2** (Fig. 1) and **3** (Fig. 2) are centrosymmetric dimers formed by bridging benzoate ligands. The Mg-O(benzoate) distances are almost the same in both molecules [O(1)-Mg(1) 1.972(1) (**2**) and 1.949(1) (**3**); O(2)-Mg(1a) 1.9563(19) (**2**) and 1.951(2) Å (**3**)], but are significantly shorter than the respective Mg-O(THF) bonds [2.144(2) (**2**), 2.1030(18) Å (**3**)].

The Mg atoms in **2** and **3** are coordinated in a slightly distorted trigonal-bipyramidal fashion. In **2** the axial positions are occupied by the THF oxygen atom O(3) and by N(2), in **3** by the THF oxygen atom O(3) and by N(1). Due to the different coordination sites of the two nitrogen atoms in **2**, the Mg-N distances show different lengths (equatorial Mg(1)-N(1) 2.115(2), axial Mg(1)-N(2) 2.185(2) Å). The difference of the Mg-N distances in **3** is remarkably higher (Mg(1)-N(1) 2.2291(18), Mg(1)-N(2) 2.0946(19) Å), since in addition to the difference in the coordination

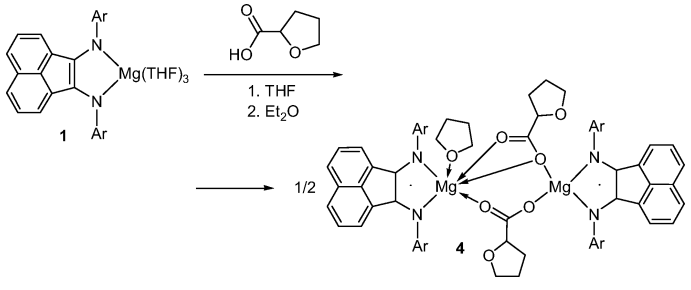

Scheme 7. Reaction route for the synthesis of **4** (Ar = 2,6-*i*Pr$_2$C$_6$H$_3$).

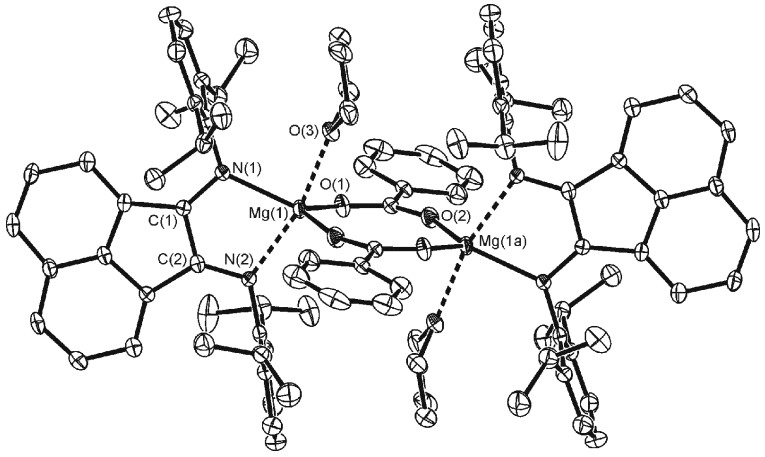

Fig. 1. ORTEP [12] presentation of the molecular structure of **2** (30 % probability ellipsoids; hydrogen atoms omitted for clarity). Selected bond lengths (Å) and angles (deg): C(1)-N(1) 1.335(3), C(1)-C(2) 1.441(3), C(2)-N(2) 1.338(3), O(1)-Mg(1) 1.9720(19), O(2)-Mg(1) 1.9563(19), O(3)-Mg(1) 2.144(2), Mg(1)-N(1) 2.115(2), Mg(1)-N(2) 2.185(2); O(1)-Mg(1)-O(2) 117.16(8), O(1)-Mg(1)-O(3) 89.60(8), O(2)-Mg(1)-O(3) 86.60(8), O(2)-Mg(1)-N(1) 125.82(9), O(1)-Mg(1)-N(1) 116.54(8), N(1)-Mg(1)-O(3) 87.15(8), N(2)-Mg(1)-O(3) 166.00(8), O(2)-Mg(1)-N(2) 98.55(8), O(1)-Mg(1)-N(2) 99.45(8), N(1)-Mg(1)-N(2) 79.26(8).

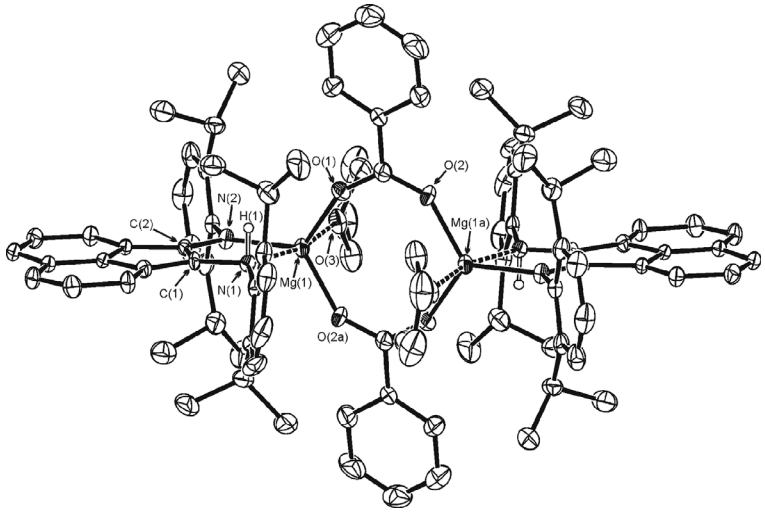

Fig. 2. ORTEP [12] presentation of the molecular structure of **3** (30 % probability ellipsoids; hydrogen atoms omitted for clarity). Selected bond lengths (Å) and angles (deg): C(1)-N(1) 1.394(2), C(1)-C(2) 1.403(3), C(2)-N(2) 1.346(2), O(1)-Mg(1) 1.9489(18), O(2)-Mg(1a) 1.951(2), O(3)-Mg(1) 2.1030(18), Mg(1)-N(1) 2.2291(18), Mg(1)-N(2) 2.0946(19); O(1)-Mg(1)-O(2a) 115.58(8), O(1)-Mg(1)-O(3) 90.25(8), O(2a)-Mg(1)-O(3) 88.51(8), O(2a)-Mg(1)-N(1) 92.73(8), O(1)-Mg(1)-N(1) 101.64(7), N(1)-Mg(1)-O(3) 166.10(7), N(2)-Mg(1)-O(3) 89.05(7), O(2a)-Mg(1)-N(2) 125.14(8), O(1)-Mg(1)-N(2) 119.23(9), N(1)-Mg(1)-N(2) 78.92(7).

site of the two nitrogen atoms, their different functionality – the Mg(1)-N(1) bond is a coordinative amino bond, the Mg(1)-N(2) bond a metal amido bond – influences the distances. The slight deviation of the N(1) atom from the geometry of a trigonal bipyramid towards a pyramidal geometry reflects the presence of the proton on this nitrogen atom. The eight-membered metallacycles in **2** and **3** are almost planar. As indicated by the dihedral angles Mg(1)-O(1)-O(2)-Mg(1a) of 15.8 (**2**) and 11.5° (**3**), they show little tendency to adopt a chair conformation. The Mg(1)···Mg(1a) separation in **2** and **3** is 4.236 and 4.296 Å, respectively.

The Mg-O(benzoate) distances in **2** and **3** compare well with those in other magnesium carboxylates [13], like in dimeric $[BrMg(OCOPh)(THF)_2]_2$ (1.983(4) and 1.930(4) Å) which also shows trigonal-bipyramidally coordinated magnesium atoms.

The results of the crystallographic structure determination of **4** proved that in contrast to the reaction of **1** with benzoic acid affording compound **3**, the reaction with furanyl-2-carboxylic acid does not proceed with protonation of the dpp-BIAN ligand, but with formation of a dinuclear dpp-BIAN-coordinated magnesium furanyl-2-carboxylate accompanied by liberation of hydrogen. In contrast to **2** and **3**, the coordination modes of the two carboxylate ligands in **4** are different (Fig. 3). The geometry of the ligand arrangement around Mg(1) is that of a trigonal bipyramid with the atoms O(1), O(5) and N(2) forming the equatorial plane (sum of the bond angles 359.8°) and the atoms N(1) and O(7) occupying the apical positions (angle N(1)-Mg(1)-O(7) 172.3°). The geometry of the ligand atoms coordinating Mg(2) is that of a tetrahedron.

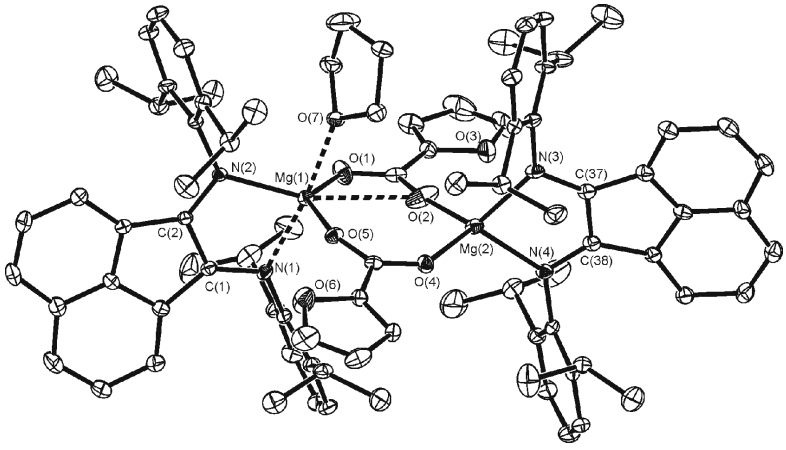

Fig. 3. ORTEP [12] presentation of the molecular structure of **4** (30 % probability ellipsoids; hydrogen atoms omitted for clarity). Selected bond lengths (Å) and angles (deg): C(1)-N(1) 1.337(3), C(2)-N(2) 1.336(3), C(1)-C(2) 1.440(3), C(37)-N(3) 1.338(3), C(38)-N(4) 1.339(3), C(37)-C(38) 1.448(3), N(1)-Mg(1) 2.163(2), N(2)-Mg(1) 2.108(2), N(3)-Mg(2) 2.082(2), N(4)-Mg(2) 2.057(2), O(1)-Mg(1) 2.030(2), O(2)-Mg(2) 1.899(2), O(4)-Mg(2) 1.9362(19), O(2)-Mg(1) 2.812(2), O(5)-Mg(1) 1.9861(19), O(7)-Mg(1) 2.1281(17); O(1)-Mg(1)-O(5) 134.71(9), N(2)-Mg(1)-O(5) 108.38(8), O(1)-Mg(1)-N(2) 116.67(9), O(5)-Mg(1)-O(7) 87.84(7), O(1)-Mg(1)-O(7) 86.33(7), N(1)-Mg(1)-O(1) 94.55(8), N(1)-Mg(1)-O(5) 96.89(8), N(1)-Mg(1)-O(7) 172.31(8), N(1)-Mg(1)-N(2) 80.81(8), N(2)-Mg(1)-O(7) 91.96(8), O(2)-Mg(2)-O(4) 103.63(10), O(2)-Mg(2)-N(3) 118.26(10), O(2)-Mg(2)-N(4) 118.93(9), O(4)-Mg(2)-N(3) 115.12(8), O(4)-Mg(2)-N(4) 116.74(9), N(4)-Mg(2)-N(3) 84.32(9).

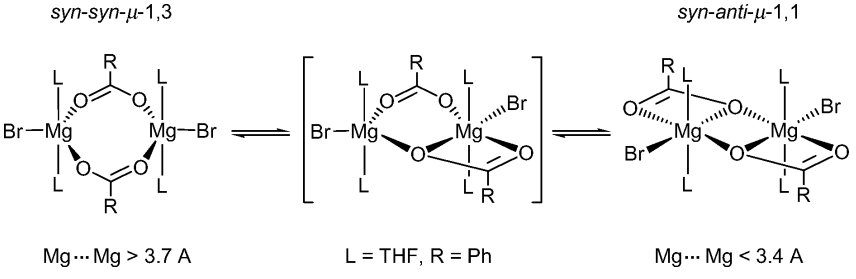

Scheme 8. Fluxional behavior of carboxylate-bridged magnesium compounds in solution.

Recently, Caudle *et al.* observed a fluxional behavior of carboxylate-bridged magnesium compounds in solution based on a bridge-mode isomerization between molecules with *syn-syn*-μ-1,3 and *syn-anti*-μ-1,1 arranged carboxylate groups (Scheme 8). Both isomers differ with respect to the distance between the two bridged magnesium atoms with larger values for the *syn-syn*-μ-1,3 isomer compared to the *syn-anti*-μ-1,1 isomer.

To the best of our knowledge, the molecules of complex **4** are the first crystallographically confirmed examples showing a configuration intermediate between *syn-syn*-μ-1,3 and *syn-anti*-μ-1,1 configurated carboxylate-bridged magnesium complexes and, as predicted, the Mg(1)···Mg(2a) distance in **4** (4.030 Å) is *ca.* 0.2 Å smaller than in the *syn-syn*-μ-1,3 configurated **2** (4.236 Å).

The four Mg-O(benzoate) distances in **4** range from 1.899(2) to 2.030(2) Å with the two shortest bonds (Mg(2)-O(2) 1.899(2) and Mg(2)-O(4) 1.936(1) Å) directed to the same magnesium atom [Mg(2)]. By comparison, the Mg(1)-O(benzoate) bond lengths are remarkably longer (Mg(1)-O(1) 2.030(2) and Mg(1)-O(5) 1.986(1) Å). The Mg(1)···O(2) distance (2.812(2) Å) suggests an interaction between these two atoms.

Probably due to the lower coordination number of Mg(2) compared to Mg(1), the Mg(2)-N(3) and Mg(2)-N(4) bonds (2.082(2) and 2.057(2) Å, respectively) are shorter than the Mg(1)-N(1) and Mg(1)-N(2) bonds (2.163(2) and 2.108(2) Å, respectively). Based on the fact that Mg(2) forms the two shortest Mg-O(benzoate) bonds, the structure of **4** may be considered as an ion pair in which the an-

ion $[(\text{dpp-BIAN})\text{Mg}\{\text{OCO}(\text{OC}_4\text{H}_3)\}_2]^-$ contacts the cation $[(\text{dpp-BIAN})\text{Mg}(\text{THF})]^+$.

The X-ray diffraction data also give information on the oxidation state of the dpp-BIAN ligand in **2**, **3** and **4**. According to the LUMO symmetry, the C(1)–N(1) and C(2)–N(2) distances should be elongated on going from neutral dpp-BIAN to its radical-anion and further to its dianion. On the other hand, the C(1)-C(2) bond length should decrease in the same order. In agreement with the expectations, the C-N bonds of **2** (C(1)–N(1) 1.340(6), C(2)–N(2) 1.332(5) Å) and **4** (C(1)-N(1) 1.337(3), C(2)-N(2) 1.336(3), C(37)-N(3) 1.338(3), C(38)-N(4) 1.339(3) Å) containing radical anionic dpp-BIAN are longer than in free dpp-BIAN (both 1.282(4) Å) [14], but shorter than in **1** (1.401(6) and 1.378(7) Å) [4]. Concerning the C-C bonds within the metallacycles it is to note that the C(1)-C(2) bond in **3** (1.403(3) Å) is shortened compared to the corresponding bonds in **2** (1.441(3) Å) and **4** (1.440(3) and 1.448(3) Å) showing a value close to that of the dpp-BIAN dianion in **1** (1.389(7) Å). This effect may be due to the fact that the dpp-BIAN dianions are bonded to the two cations $[\text{Mg}(\text{OCOR})]^+$ and to H^+. Since the proton at the N(1) atom could not be detected by difference Fourier syntheses and the position of N(1) as top of a pyramide is not very pronounced, a comparison of the C-N bond lengths within the metallacycle of **3** with those in the complexes depicted in Scheme 4 is helpful in the discussion whether complex **3** contains a protonated dpp-BIAN ligand. From the facts that the C-N(Mg) and the C-N(H) bonds show different lengths (C(2)-N(2) 1.346(2) Å, C(1)-N(1) 1.394(2) Å) as it is the case in $[(\text{dpp-BIAN})(\text{H})]\text{Mg}(\text{CCPh})(\text{THF})_2$ (N(1)-C(1) 1.444(3), N(2)-C(2) 1.350(3) Å) [11a], and that the ^{1}H NMR spectrum of **3** in $[\text{D}_8]$-THF shows a singlet signal for one proton in the region expected for nitrogen-bonded hydrogen atoms at δ = 5.84 ppm, we conclude that complex **3** contains the protonated dpp-BIAN ligand.

Experimental Section

All manipulations were carried out in vacuum using standard Schlenk techniques. The solvents THF and benzene were distilled from sodium/benzophenone prior to use. Freshly sublimed benzoyl peroxide and furanyl-2-carboxylic acid were used for the reactions. The IR-spectra were recorded using an FTIR FSM-1201 spectrometer, the ^{1}H NMR spectrum of **3** using a Bruker DPX 200 spectrometer. Solutions of **1** were prepared as described below following the method given in the literature [4] and were used *in situ*. The yields of the complexes are calculated on the basis of the amount of dpp-BIAN used in the reactions.

*(dpp-BIAN)Mg(THF)$_3$ (**1**)*

Magnesium shavings (2.4 g, 100 mmol) and I_2 (0.25 g, 1.0 mmol) were placed in a Schlenk-like ampoule (*ca.* 100 mL volume) equipped with a Teflon stopcock. After evacuation of the ampoule, THF (40 mL) was added by condensation and the mixture was stirred for 2 h. The $\text{MgI}_2(\text{THF})_n$ formed and the solvent were separated by decantation, and the residual metal was washed with THF (40 mL). Then a suspension of dpp-BIAN (0.5 g, 1.0 mmol) in THF (30 mL) was added to the activated magnesium metal, and the mixture was refluxed. In the course of about 10 min, the reaction mixture turned deep green. The solution was then cooled to ambient temperature, decanted from the excess of magnesium and used *in situ* for the synthesis of **2**, **3** and **4**.

*[(dpp-BIAN)MgOCOPh(THF)]$_2$ (**2**)*

To the THF solution of **1**, prepared as described above, 0.12 g (0.5 mmol) of benzoyl peroxide was added with stirring. The reaction mixture instantly turned cherry-red. Reduction of the volume of the solution by evaporation of the solvent in a vacuum and cooling of the remaining solution (*ca.* 7 mL) caused the separation of red-brown crystals of **2** (0.51 g, 64 %). M. p. 157 °C. – IR (nujol): ν = 1720 (m), 1668 (m), 1627 (s), 1616 (s), 1602 (s), 1573 (s), 1536 (s), 1445 (s), 1428 (s), 1361 (w), 1318 (m), 1278 (w), 1252 (m), 1220 (w), 1186 (m), 1179 (m), 1159 (w), 1069 (s), 1046 (s), 1024 (m), 1012 (w), 962 (w), 939 (m), 911 (s), 885 (w), 859 (m), 818 (m), 804 (m), 790 (m), 669 (w), 581 (m), 480 (m) cm^{-1}. – $\text{C}_{102}\text{H}_{122}\text{Mg}_2\text{N}_4\text{O}_8$ (1580.66): calcd. C 77.50, H 7.78; found C 77.17, H 7.34.

*[(dpp-BIAN)(H)MgOCOPh(THF)]$_2$ (**3**)*

To the THF solution of **1**, prepared as described above, 0.122 g (1 mmol) of benzoic acid was added with stirring. The color of the reaction mixture turned from green to deep blue. After filtration of the solution, the solvent THF was evaporated in a vacuum and the residue was redissolved in Et_2O (*ca.* 20 mL). Cooling of this solution caused separation of deep blue crystals of **3** (0.37 g, 60 %). M. p. > 220 °C. – IR (nujol): ν = 1626 (s), 1617 (s), 1574 (s), 1527 (s), 1442 (s), 1317 (m), 1249 (m), 1221 (w), 1187 (m), 1153 (w), 1119 (m), 1079 (w), 1044 (m), 961 (w), 936 (w), 911 (m), 858 (w), 845 (w), 817 (m), 802 (m), 765 (s), 741 (w), 669 (w), 620 (w), 585 (w), 543 (w), 475 (m), 411 (s) cm^{-1}. – ^{1}H NMR (200 MHz, $[\text{D}_8]$-THF, 20 °C): δ = 7.7 – 7.0 (m, 15 H, CH arom.), 6.93 (t, J = 8.0, 1 H, CH arom.), 6.09 (d, J = 6.8, 1 H, CH arom.), 5.84 (s, 1 H, NH), 3.67 – 3.59 (m, 4 H, C*H*$(\text{CH}_3)_2$), 3.40 (q, J = 7.0, 8 H, O*CH*$_2$CH$_3$), 1.23 (d, J = 7.0, 12 H, CH(C*H*$_3$)CH$_3$), 1.15 (d, J = 7.0, 12 H, CH(C*H*$_3$)CH$_3$), 1.09 (t, J = 7.0, 12 H,

Table 1. Parameters of the single crystals, data collection and structure refinement of **2** – **4**.

Compound	**2**	**3**	**4**
Empirical formula	$C_{102}H_{122}Mg_2N_4O_8$	$C_{102}H_{128}Mg_2N_4O_8$	$C_{86}H_{94}Mg_2N_4O_7$
Formula weight, g mol^{-1}	1580.66	1586.70	1344.27
Crystal size, mm^3	$0.14 \times 0.08 \times 0.08$	$0.10 \times 0.10 \times 0.10$	$0.21 \times 0.20 \times 0.20$
Crystal system	triclinic	triclinic	monoclinic
Space group	$P\bar{1}$	$P\bar{1}$	$P2_1/c$
Z	1	1	4
a, Å	12.748(3)	12.7044(8)	25.1865(8)
b, Å	13.4964(18)	13.7447(12)	12.3241(3)
c, Å	14.592(5)	14.5443(9)	25.7479(7)
α, deg	114.10(2)	65.163(7)	90.00
β, deg	95.48(2)	80.187(5)	111.669(3)
γ, deg	93.002(14)	86.212(6)	90.00
V, Å^3	2269.6(10)	2271.0(3)	7427.4(4)
F(000), e	850	856	2872
D_c, g cm^{-3}	1.156	1.160	1.202
Abs. coefficient, mm^{-1}	0.084	0.085	0.091
Max./min. transmission	0.993/0.988	0.979/0.983	0.993/0.988
2θ range for data collection, deg	$2.95 \leq \theta \leq 28.68$	$2.98 \leq \theta \leq 27.50$	$2.94 \leq \theta \leq 28.85$
Data set	$-16 \leq h \leq 15$	$-16 \leq h \leq 16$	$-33 \leq h \leq 34$
	$-17 \leq k \leq 17$	$-17 \leq k \leq 17$	$-15 \leq k \leq 15$
	$-18 \leq l \leq 19$	$-18 \leq l \leq 18$	$-32 \leq l \leq 34$
Reflections, collected	21833	21629	48746
Reflections, unique	9911	10010	17054
R_{int}	0.041	0.074	0.075
Data/restraints/parameter	9911/0/489	10010/0/533	17054/0/908
Goodness-of-fit (F^2)	0.934	0.667	0.968
Final R indices [$I \geq 2\sigma(I)$]	$R1 = 0.058$	$R1 = 0.047$	$R1 = 0.066$
	$wR2 = 0.155$	$wR2 = 0.069$	$wR2 = 0.094$
R indices (all data)	$R1 = 0.122$	$R1 = 0.0207$	$R1 = 0.175$
	$wR2 = 0.174$	$wR2 = 0.084$	$wR2 = 0.122$
$\Delta\rho_{fin}$ (max/min), e Å^{-3}	0.31/−0.26	0.23/−0.27	0.47/−0.46

OCH_2CH_3) ppm. – $C_{102}H_{128}Mg_2N_4O_8$ (1586.70): calcd. C 77.21, H 8.13; found C 77.14, H 7.98.

*(dpp-BIAN)Mg[OCO(2-C$_4$H$_3$O)]$_2$Mg(dpp-BIAN)(THF) (**4**)*

To the THF solution of **1**, prepared as described above, 0.12 g (1 mmol) of furanyl-2-carboxylic acid was added with stirring. The color of the reaction mixture turned from green-brown to grayish-green. Then the THF was evaporated in a vacuum. Recrystallization of the residue from benzene (*ca.* 5 mL) afforded red crystals of **4** (0.33 g, 49 %). M. p. > 213 °C. – IR (nujol): ν = 1619 (s), 1584 (s), 1552 (s), 1488 (s), 1419 (s), 1361 (m), 1318 (m), 1253 (m), 1226 (m), 1203 (m), 1184 (s), 1142 (m), 1076 (s), 1057 (w), 1034 (m), 1011 (s), 938 (s), 880 (s), 853 (m), 819 (s), 800 (m), 788 (m), 757 (s), 672 (w), 615 (w), 592 (w), 542 (w), 499 (s), 453 (m), 419 (s) cm^{-1}. – $C_{86}H_{94}Mg_2N_4O_7$ (1344.27): calcd. C 76.84, H 7.05; found C 76.40, H 7.02.

Crystal structure determination

Crystals suitable for X-ray diffraction were obtained by crystallization from THF (**2**), diethyl ether (**3**), and benzene (**4**). The data were collected using an Xcalibur S Sapphire diffractometer (Oxford Diffraction) at 150 K. The structures were solved by Direct Methods using SIR97 [15] or SIR2004 [16] and were refined on F^2 using all reflections with SHELXL-97 [17]. All non-hydrogen atoms were refined anisotropically and the carbon-bonded hydrogen atoms were placed in calculated positions using a riding model. SADABS [18] was used to perform area-detector scaling and absorption corrections. The important parameters of the single crystals, the data collection and the refinement data of the structures are listed in Table 1.

CCDC-655391 (**2**), CCDC-657435 (**3**), and CCDC-655392 (**4**) contain the supplementary crystallographic data for this paper. These data can be obtained free of charge from the Cambridge Crystallographic Data Centre *via* www.ccdc.cam.ac.uk/data_request/cif.

Acknowledgement

This work was supported by the Alexander von Humboldt Foundation (Partnership Project between the IOMC RAS and the Institut für Chemie der Technischen Universität Berlin), the Russian Foundation for Basic Research (Grant No. 07-03-00545), and the Fonds der Chemischen Industrie.

[1] a) G. A. Abakumov, V. I. Nevodchikov, V. K. Cherkasov, *Dokl. Akad Nauk SSSR* **1984**, *278*, 641; b) G. A. Abakumov, G. A. Razuvaev, V. I. Nevodchikov, V. K. Cherkasov, *J. Organomet. Chem*. **1988**, *341*, 485; c) C. W. Lange, M. Foldeaki, V. I. Nevodchikov, K. Cherkasov, G. A. Abakumov, C. G. Pierpont, *J. Am. Chem. Soc*. **1992**, *114*, 4220; d) G. A. Abakumov, V. K. Cherkasov, M. P. Bubnov, O. G. Ellert, Zh. V. Dobrokhotova, L. N. Zakharov, Yu. T. Struchkov, *Dokl. Akad. Nauk* **1993**, *328*, 332; e) G. A. Abakumov, V. K. Cherkasov, V. I. Nevodchikov, V. A. Kuropatov, G. T. Yee, C. G. Pierpont, *Inorg. Chem*. **2001**, *40*, 2434.

[2] a) G. A. Abakumov, A. I. Poddel'sky, E. V. Grunova, V. K. Cherkasov, G. K. Fukin, Yu. A. Kurskii, L. G. Abakumova, *Angew. Chem*. **2005**, *117*, 2827; *Angew. Chem. Int. Ed*. **2005**, *44*, 2767; b) G. A. Abakumov, V. K. Cherkasov, E. V. Grunova, A. I. Poddel'skii, L. G.Abakumova, Yu. A. Kurskii, G. K. Fukin, E. V. Baranov, *Dokl. Chem*. **2005**, *405*, 222; c) V. K. Cherkasov, G. A. Abakumov, E. V. Grunova, A. I. Poddel'sky, G. K. Fukin, E. V. Baranov, Yu. A. Kurskii, L. G. Abakumova, *Chem. Eur. J*. **2006**, *12*, 3916.

[3] a) I. L. Fedushkin, A. A. Skatova, V. A. Chudakova, G. K. Fukin, *Angew. Chem*. **2003**, *115*, 3416; *Angew. Chem. Int. Ed*. **2003**, *42*, 3294; b) I. L. Fedushkin, A. A. Skatova, V. A. Chudakova, V. K. Cherkasov, G. K. Fukin, M. A. Lopatin, *Eur. J. Inorg. Chem*. **2004**, 388;

[4] I. L. Fedushkin, A. A. Skatova, V. A. Chudakova, G. K. Fukin, S. Dechert, H. Schumann, *Eur. J. Inorg. Chem*. **2003**, 3336.

[5] A. N. Lukoyanov, I. L. Fedushkin, M. Hummert, H. Schumann, *Russ. Chem. Bull*. **2006**, *55*, 422.

[6] a) H. Schumann, M. Hummert, A. N. Lukoyanov, I. L. Fedushkin, *Organometallics* **2005**, *24*, 3891; b) A. N. Lukoyanov, I. L. Fedushkin, H. Schumann, M. Hummert, *Z. Anorg. Allg. Chem*. **2006**, *632*, 1471; H. Schumann, M. Hummert, A. N. Lukoyanov, I. L. Fedushkin, *Chem. Eur. J*. **2007**, *13*, 4216.

[7] a) I. L. Fedushkin, A. A. Skatova, V. A. Chudakova, N. M. Khvoinova, A. Yu. Baurin, D. Sebastian, M. Hummert, H. Schumann, *Organometallics* **2004**, *23*, 3714; b) I. L. Fedushkin, N. M. Khvoinova, A. Yu. Baurin, G. K. Fukin, V. K. Cherkasov, M. P. Bubnov, *Inorg. Chem*. **2004**, *43*, 7807; c) I. L. Fedushkin, N. M. Khvoinova, A. Yu. Baurin, V. A. Chudakova, A. A. Skatova, V. K. Cherkasov, G. K. Fukin, E. V. Baranov, *Russ. Chem. Bull*. **2006**, *55*, 74; d) I. L. Fedushkin, M. Hummert, H. Schumann, *Eur. J. Inorg. Chem*. **2006**, 3266.

[8] I. L. Fedushkin, A. A. Skatova, V. K. Cherkasov, V. A. Chudakova, S. Dechert, M. Hummert, H. Schumann, *Chem. Eur. J*. **2003**, *9*, 5778.

[9] a) I. L. Fedushkin, A. A. Skatova, A. N. Lukoyanov, V. A. Chudakova, S. Dechert, M. Hummert, H. Schumann, *Russ. Chem. Bull*. **2004**, *53*, 2751; b) I. L. Fedushkin, V. M. Makarov, E. C. E. Rosenthal, G. K. Fukin, *Eur. J. Inorg. Chem*. **2006**, 827.

[10] I. L. Fedushkin, A. A. Skatova, M. Hummert, H. Schumann, *Eur. J. Inorg. Chem*. **2005**, 1601.

[11] a) I. L. Fedushkin, N. M. Khvoinova, A. A. Skatova, G. K. Fukin, *Angew. Chem*. **2003**, *115*, 5381; *Angew. Chem. Int. Ed*. **2003**, *42*, 5223; b) I. L. Fedushkin, A. A. Skatova, G. K. Fukin, M. Hummert, H. Schumann, *Eur. J. Inorg. Chem*. **2005**, 2332; c) I. L. Fedushkin, A. G. Morozov, O. V. Rassadin, G. K. Fukin, *Chem. Eur. J*. **2005**, *11*, 5749.

[12] A. L. Spek, PLATON, A. Multipurpose Crystallographic Tool, Utrecht University, Utrecht (The Netherlands) **2000**. See also: A. L. Spek, *J. Appl. Cryst*. **2003**, *36*, 7 – 13.

[13] a) J. W. Yun, T. Tanase, S. J. Lippard, *Inorg. Chem*. **1996**, *35*, 7590; b) B. Paluchowska, J. K. Maurin, J. Leciejewicz, *J. Chem. Crystallogr*. **1997**, *27*, 177; c) K.-C. Yang, C.-C. Chang, C-S. Yeh, G.-H. Lee, S.-M. Peng, *Organometallics* **2001**, *20*, 126; d) K.-C. Yang, C.-C. Chang, C.-S. Yeh, G.-H. Lee, Y. Wang, *Organometallics* **2002**, *21*, 1296; e) A. P. Dove, V. C. Gibson, P. Hormnirun, E. L. Marshall, J. A. Segal, A. J. P. White, D. J. Williams, *Dalton. Trans*. **2003**, 3088; f) M. T. Caudle, W. W. Brennessel, V. G. Young, Jr., *Inorg. Chem*. **2005**, *44*, 3233; g) R. P. Davies, R. J. Less, P. D. Lickiss, A. J. P. White, *Dalton Trans*. **2007**, 2528.

[14] I. L. Fedushkin, V. A. Chudakova, G. K. Fukin, S. Dechert, M. Hummert, H. Schumann, *Russ. Chem. Bul. Int. Ed*. **2004**, *53*, 2744.

[15] A. Altomare, M. C. Burla, M. Camalli, G. L. Cascarano, C. Giacovazzo, A. Guagliardi, A. G. C. Moliterni, G. Polidori, R. Spagna, SIR97, *J. Appl. Crystallogr*. **1999**, *32*, 115.

[16] M. C. Burla, R. Caliandro, M. Camalli, B. Carrozzini, G. L. Cascarano, L. de Caro, C. Giacovazzo, G. Polidori, R. Spagna, SIR2004, *J. Appl. Cryst*. **2005**, *38*, 381.

[17] G. M. Sheldrick, SHELXL-97, Program for the Refinement of Crystal Structures, University of Göttingen, Göttingen (Germany) **1997**.

[18] G. M. Sheldrick, SADABS, Program for Empirical Absorption Correction of Area Detector Data, University of Göttingen, Göttingen (Germany) **1996**.